



OPEN ACCESS

EDITED BY

Takahisa Hiramitsu,
Japanese Red Cross Nagoya Daini Hospital,
Japan

REVIEWED BY

Massimo Procopio,
Molinette Hospital, Italy
Alfredo Adolfo Reza-Albarrán,
National Institute of Medical Sciences and
Nutrition Salvador Zubirán, Mexico

*CORRESPONDENCE

Jian He

✉ hjxueren@126.com

Jing Yao

✉ jingyao@nju.edu.cn

Zhengyang Zhou

✉ zyzhou@nju.edu.cn

RECEIVED 02 December 2024

ACCEPTED 14 March 2025

PUBLISHED 04 April 2025

CITATION

Liu C, Li M, Li W, Xue H, Zhang Y, Wei S, He J,
Yao J and Zhou Z (2025) A retrospective
study on a nomogram combining clinical and
ultrasound parameters for differentiating
solitary parathyroid adenoma from
carcinoma or atypical tumors.
Front. Endocrinol. 16:1538361.
doi: 10.3389/fendo.2025.1538361

COPYRIGHT

© 2025 Liu, Li, Li, Xue, Zhang, Wei, He, Yao and
Zhou. This is an open-access article distributed
under the terms of the [Creative Commons
Attribution License \(CC BY\)](#). The use,
distribution or reproduction in other forums
is permitted, provided the original author(s)
and the copyright owner(s) are credited and
that the original publication in this journal is
cited, in accordance with accepted academic
practice. No use, distribution or reproduction
is permitted which does not comply with
these terms.

A retrospective study on a nomogram combining clinical and ultrasound parameters for differentiating solitary parathyroid adenoma from carcinoma or atypical tumors

Chunrui Liu¹, Mingxia Li¹, Wenxian Li¹, Haiyan Xue¹,
Yidan Zhang¹, Shuping Wei¹, Jian He^{2*}, Jing Yao^{2*}
and Zhengyang Zhou^{3*}

¹Department of Ultrasound, Nanjing Drum Tower Hospital, Affiliated Hospital of Medical School, Nanjing University, Nanjing, Jiangsu, China, ²Department of Nuclear Medicine, Nanjing Drum Tower Hospital, Affiliated Hospital of Medical School, Nanjing University, Nanjing, China, ³Department of Radiology, Nanjing Drum Tower Hospital, Affiliated Hospital of Medical School, Nanjing University, Nanjing, China

Objective: Parathyroid carcinoma (PC) and atypical parathyroid tumor (APT) are rare malignant parathyroid disorders with varying degrees of recurrence risk. The aim of this study was to determine an effective model for discriminating PC/APT among solitary parathyroid lesions.

Methods: A total of 439 patients with histologically confirmed primary hyperparathyroidism were retrospectively enrolled. The training cohort comprised 207 patients, the validation cohort comprised 52 patients from Hospital I, and the external validation cohort comprised 180 patients from Hospital II. All patients were diagnosed in the parathyroid adenoma (PA) group and the APT/PC group. The clinical and ultrasonic features of the two patient groups were compared. Multivariate logistic regression analysis was conducted to identify independent risk factors for APT/PC. A nomogram was built based on multivariate logistic regression analysis. Model discrimination was assessed using receiver operating characteristic (ROC) curve analysis. The area under the curve (AUC), sensitivity, specificity, and accuracy were reported. Decision and calibration curve analyses were performed to assess the clinical value and calibration of each model, respectively.

Results: In the training set, there were 181 cases of PA and 26 cases of APC/PC. Intact parathyroid hormone (iPTH) [odds ratio (OR): 1.019, 95% confidence interval (CI): 1.008–1.032], shape (OR: 16.625, 95% CI: 5.922–51.883), and relation with the thyroid capsule (OR: 3.422, 95% CI: 1.455–9.152) were independent predictive factors associated with the risk of APT/PC. The AUCs for training and internal and external validation were 0.929, 0.962, and 0.965, respectively. The accuracy, sensitivity, and specificity were 86%, 96%, and 85% in the training cohort; 92%, 100%, and 90% in the validation cohort; and 88%, 100%, and 88% in the external validation cohort, respectively. In addition, calibration plots graphically showed good agreement in the presence of the APT/PC group

between risk estimation by the nomogram and histopathologic confirmation of surgical specimens. DCA in the current study showed that the nomogram was more effective than all-patient treatment or no treatment over a wide range of threshold probabilities.

Conclusions: Ultrasonic features in combination with iPTH levels may be an applicable model for predicting potentially malignant parathyroid tumors and has a better potential to facilitate preoperative decision-making.

KEYWORDS

parathyroid neoplasms, parathyroid carcinoma, ultrasonography, nomograms, primary hyperparathyroidism

1 Introduction

Parathyroid neoplasms are a heterogeneous group of tumors affecting 0.1%–5.0% of the global population (1). Patients often present with hyperparathyroidism and hypercalcemia. The 2022 World Health Organization (WHO) classification classifies parathyroid neoplasms into parathyroid adenoma (PA), atypical parathyroid tumors (APTs), and parathyroid carcinoma (PC) (2). Approximately 85% of patients harbor a single PA and can be treated conservatively or with minimally invasive parathyroidectomy (MIP) (3). APT and PC are comparatively rare, comprising 0.5%–5% of patients in Western countries but up to 6%–11.5% in Asian countries (4–6). *En bloc* resection, but not local excision, is often required for APT and PC (7). APT and PC exhibit similar aggressive characteristics in routine histopathology. However, APT lacks the complete capsular or vascular invasion observed in PC (8). Clinically, both APT and PC patients require frequent follow-up to detect regional or distant metastasis (9). Approximately 60% of PC patients face repeated recurrence or metastasis, leading to fatal hypercalcemia (4, 10). Preoperative identification of such aggressive parathyroid tumors and extensive neck surgery is important for patient prognosis.

Typical PA, APT, or PC exhibits similar or overlapping clinical symptoms. These symptoms include nephrolithiasis, bone and joint pain, fatigue, weakness, anxiety, and mood disturbances. However, some individuals may be asymptomatic (5). High parathyroid hormone (PTH), alkaline phosphatase (ALP), and 24-h urinary calcium excretion levels may be predictive of carcinoma (11). Schulte et al. found that parathyroid lesions <3 cm in patients with serum calcium levels <3 mmol/L are rarely malignant if other cancer-indicative features are absent (7). However, relying solely on the preoperative biochemical or clinical manifestations makes preoperative differentiation challenging. Moreover, preoperative biopsy is not recommended for parathyroid neoplasms because of the risk of neoplastic cells and influence of surgical pathology (4, 7). Hence, there is an urgent need for precise and efficient imaging markers for the preoperative classification of malignant or potentially malignant lesions.

Cervical ultrasonography (US) and [^{99m}Tc] Tc-MIBI scintigraphy are recommended for localizing parathyroid neoplasms and determining the optimal surgical approach (12). High-resolution ultrasound imaging is highly accessible, is cost-effective, and does not involve exposure to radiation. Certain US characteristics may facilitate preoperative identification of malignant lesions, including irregular margins, heterogeneous echotexture, intranodular calcifications, indistinct capsule boundaries, and chaotic and heterogeneous vasculature (13). However, the value of ^{99m}Tc sestamibi (MIBI) in distinguishing benign from malignant parathyroid lesions is limited because of its lack of specificity (14). Computed tomography (CT) scans help detect parathyroid masses, infiltration of surrounding structures, and distant metastases (15). [¹⁸F]-Fluorocholine PET/CT (FCH-PET) has the best advantage of localizing hyperfunctional parathyroids (16); however, the value of the differential diagnosis of parathyroid lesions is unknown. Thus, compared with other diagnostic techniques, ultrasound is a promising tool for predicting the potential malignancy of parathyroid lesions.

Several studies have developed ultrasound methods to predict the potential malignancy of parathyroid lesions (17–19). Liu et al. found (17) that DR (two diameters' ratio of the lesion) and tumor infiltration in conjunction with intact parathyroid hormone (iPTH) level were independent predictors of PC. Liu et al. (18) also found that the “colored lesion” and “stiff rim” patterns on the elastogram are more indicated in PC and APT. Zhou et al. (19) developed an explainable machine learning model for the identification of hyper-functioning parathyroid glands. These studies are frequently constrained by their limited sample sizes and single-center data collection, as well as the utilization of sophisticated machine learning and elastography techniques, which impede the broad generalization of their findings. Herein, we conducted a retrospective study employing available clinical and ultrasonographic features and developed a predictive nomogram to differentiate PA from APT/PC in solitary parathyroid neoplasms.

2 Materials and methods

2.1 Patients

This retrospective study enrolled a total of 781 patients with pathologically confirmed parathyroid gland lesions, drawn from two institutions: 408 patients from institution 1 and 373 patients from institution 2. The inclusion criteria were as follows: (a) primary hyperparathyroidism (PHPT) diagnosis required persistent hypercalcemia and PTH elevation after 25OHD normalization (>30 ng/mL for ≥ 4 weeks); (b) US examination before surgery; (c) bilateral neck exploration (BNE) and MIP; (d) availability of complete clinical data; and (e) pathologically confirmed diagnosis of solitary PA, APT, or PC by a pathologist using the 2022 WHO criteria (2) and a follow-up period of at least 6 months. Exclusion criteria were as follows: (a) recurrent PHPT, secondary hyperparathyroidism (SHPT), multiple gland disease, and known multiple endocrine neoplasia/known genetic syndrome associated with PHPT; (b) absence of clinical and ultrasonic data; (c) an unclear pathological diagnosis; (d) patients with ultrasound-invisible masses; (e) unsatisfactory image quality for analysis, such as the presence of marks or artifacts in the US images; (f) patients with metastatic parathyroid cancer; and (g) patients who underwent fine-needle aspiration. The study protocol was approved by the ethics committee of the participating hospital (2024-611-01) and adhered to the principles outlined in the Declaration of Helsinki and the Good Clinical Practice guidelines (27). The requirement for informed consent from patients was waived. A flowchart outlining the study design is shown in Figure 1.

In total, 439 patients with histologically confirmed PHPT from two hospitals were included in this study between 1 January 2016 and 30 June 2024. A total of 259 patients from Hospital I (Nanjing Drum Tower Hospital) were reviewed. Patients were randomly divided into a training set and an internal validation set at a ratio of

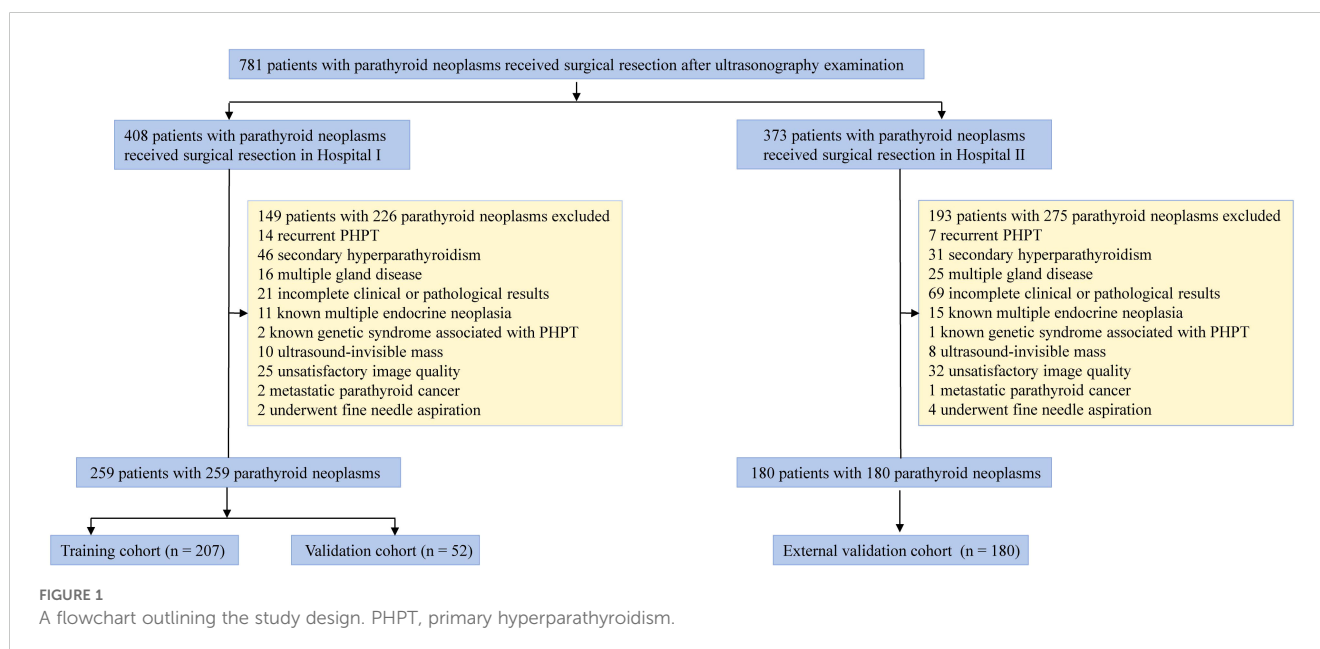
7:3. A total of 207 and 52 patients were identified as the training and validation cohorts, respectively. A total of 180 patients from Hospital II (First Affiliated Hospital of Nanjing Medical University) were recruited as the external validation cohort.

2.2 Clinical parameters

The preoperative clinical and biochemical parameters collected for analysis included age, sex, preoperative serum iPTH, and serum calcium. Serum iPTH was quantified using standardized second-generation chemiluminescent immunoassays (Siemens Centaur XP or Atellica IM platforms) targeting full-length PTH (1–84) in two hospitals. We carefully searched for the maximal calcium with concomitant PTH levels at the individual level in the patients' charts. Abnormal values were defined according to laboratory-specific reference ranges. The normal range for serum calcium at our institute is 2.25–2.75 mmol/L and that for serum iPTH is 1.31–8.14 pmol/L.

2.3 US examination and interpretation

All US examinations were conducted by four board-certified radiologists with more than 5 years of experience in superficial tissue ultrasound imaging. The equipment used included LOGIQ E9 (GE Healthcare, USA), EPIQ 5 (Philips, Netherlands), and Resona 7 (Mindray, China), with high-frequency probes. Image settings such as time-gain compensation, focal position, and dynamic range were optimized according to the manufacturer's guidelines. The patients were examined in the supine position with neck hyperextension. Scanning started from the thoracic inlet and the base of the common carotid artery origins, proceeding upward to the carotid bifurcation and submental region, including the



lateral cervical areas. US images were captured in transverse and longitudinal sections, with the largest horizontal and vertical cross-sections recorded for analysis. Vascular supply was assessed using color Doppler flow imaging (CDFI).

Two experienced radiologists (6 and 8 years, respectively) reviewed all US images; they did not participate in the image acquisition and they were blinded to clinical information and final diagnoses of each patient. Ultrasound characteristics such as size, echogenicity, shape, location, composition, vascular pattern, and visualization of the polar artery were evaluated in concordance with previous studies (20, 21). The criteria used for categorizing ultrasound features are shown in [Supplementary Table S1](#) and [Figure 2](#). A total of 50 parathyroid ultrasound images were randomly extracted. Interobserver agreement and intraobserver agreement in the radiological features were calculated to assess feature reproducibility.

2.4 Statistical analysis

Statistical analysis was performed by using SPSS (version 23.0) and R software (version 3.4.4). Categorical variables were compared using the chi-square test or Fisher's exact test, and continuous variables were compared using the Student's *t*-test or the Mann-Whitney *U* test. Interobserver agreement in the radiological features was calculated using weighted kappa statistics for categorical

variables and ICC to assess feature reproducibility. An ICC value > 0.75 was regarded as good agreement. Variables with significant differences between PA and APT/PC in the univariate analysis were subsequently included in the multivariate logistic regression analysis. Backward stepwise factor selection was performed using the Akaike information criterion. A nomogram was built based on multivariate logistic regression analysis as a graphical presentation. Model discrimination was assessed using receiver operating characteristic (ROC) curve analysis. The area under the curve (AUC), sensitivity, specificity, and accuracy were reported. Model fit was assessed using the Hosmer-Lemeshow goodness-of-fit test. Decision and calibration curve analyses were performed to assess the clinical value and calibration of each model, respectively. Two-tailed $p < 0.05$ denoted a significant difference.

3 Results

3.1 Baseline characteristics

[Table 1](#) summarizes the clinical parameters, ultrasound features, and pathological subtypes of 439 patients with parathyroid neoplasms from the two hospitals. The patients were classified into three cohorts, which consisted of a training cohort ($n = 207$), a validation cohort ($n = 52$), and an external validation

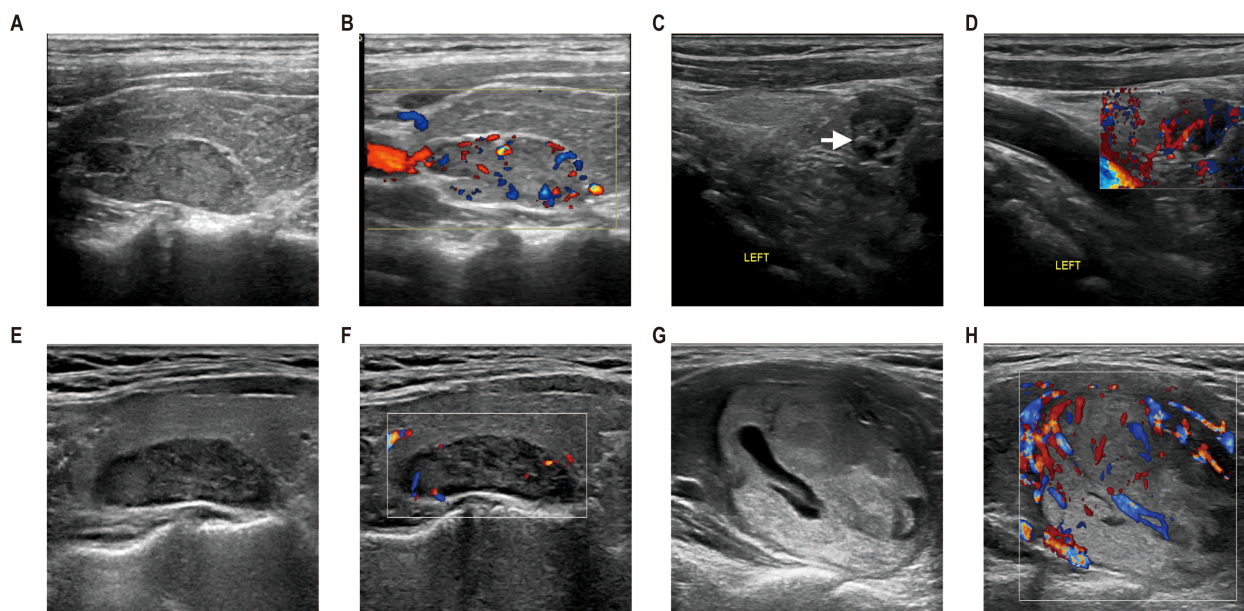


FIGURE 2

The ultrasonographic manifestations of parathyroid lesions with different pathological types. **(A, B)** Ultrasonography from a 27-year-old man with parathyroid carcinoma (PC). An isoechoic solid lesion with an incomplete capsule and irregular shape was located in the right upper parathyroid region, with the relation to the thyroid gland extending $>50\%$. Color Doppler flow imaging (CDFI) revealed polar vessels with increased mixed vascularity. **(C, D)** Ultrasonography of a 54-year-old woman with APT. A hypoechoic solid lesion with incomplete capsule, irregular shape, and internal calcification (arrows) was observed in the lower left parathyroid region, with the relation to the thyroid gland extending $\leq 50\%$. CDFI demonstrated polar vessels with increased mixed vascularity. **(E, F)** Ultrasonography of a 51-year-old woman with parathyroid adenoma. Ultrasound examination revealed a hypoechoic lesion with complete capsule and regular shape in the upper left parathyroid region. The relation to the thyroid gland extended $>50\%$. CDFI, avascularity. **(G, H)** Ultrasonography of a 49-year-old woman with parathyroid adenoma. A mixed echotexture lesion with cystic change $<50\%$ was identified in the lower left parathyroid region, exhibiting a complete capsule and regular shape. The relation to the thyroid gland extended $>50\%$. Postoperative pathology confirmed parathyroid adenoma.

TABLE 1 Participant baseline characteristics of the three cohorts.

| Characteristic | Training cohort (n = 207) | Validation cohort (n = 52) | External validation cohort (n = 180) |
|--|---------------------------|----------------------------|--------------------------------------|
| Sex, n (%) | | | |
| Male | 60 (29.0%) | 11 (21.2%) | 74 (41.1%) |
| Female | 147 (71.0%) | 41 (78.8%) | 106 (58.9%) |
| Age at diagnosis, years | 57.0 (20.0, 83.0) | 54.0 (25.0, 80.0) | 55.0 (25.0, 80.0) |
| Serum iPTH, pmol/L [M (Q ₁ , Q ₃)] | 22.5 (14.3, 33.1) | 19.0 (8.7, 140.3) | 12.3 (6.5, 212.0) |
| Serum calcium, mmol/L [M (Q ₁ , Q ₃)] | 2.9 (2.7, 3.1) | 2.9 (2.5, 4.6) | 3.0 (2.1, 4.8) |
| Size, n (%) | | | |
| <3 cm | 149 (72.0%) | 38 (72.1%) | 131 (67.8%) |
| ≥3 cm | 58 (28.0%) | 14 (26.9%) | 49 (27.2%) |
| Echo texture, n (%) | | | |
| Hypoechoic | 155 (74.9%) | 40 (76.9%) | 151 (83.9%) |
| Hyperechoic | 8 (3.9%) | 3 (5.8%) | 1 (0.6%) |
| Mixed | 44 (21.3%) | 9 (17.3%) | 28 (15.6%) |
| Capsule, n (%) | | | |
| Complete | 137 (66.2%) | 44 (84.6%) | 169 (93.9%) |
| Incomplete | 70 (33.8%) | 8 (15.4%) | 11 (6.1%) |
| Shape, n (%) | | | |
| Regular | 168 (81.2%) | 44 (84.6%) | 152 (84.4%) |
| Irregular | 39 (18.8%) | 8 (15.4%) | 28 (15.6%) |
| Location, n (%) | | | |
| Typical | 193 (93.2%) | 50 (96.2%) | 172 (95.6%) |
| Ectopic | 14 (6.8%) | 2 (3.8%) | 8 (4.4%) |
| Composition, n (%) | | | |
| Solid | 181 (87.4%) | 46 (88.5%) | 154 (85.6%) |
| Cystic component ≤ 50% | 22 (10.6%) | 6 (11.5%) | 23 (12.3%) |
| Cystic component > 50% | 4 (1.9%) | 0 | 3 (1.7%) |
| Relation with thyroid capsule, n (%) | | | |
| No-touching | 78 (37.7%) | 22 (42.3%) | 109 (60.6%) |
| Indenting ≤ 50% | 98 (47.3%) | 23 (44.2%) | 56 (31.1%) |
| Indenting > 50% | 31 (15.0%) | 7 (13.5%) | 15 (8.3%) |
| Visualization of polar artery, n (%) | | | |
| Present | 149 (72.0%) | 33 (63.5%) | 93 (51.7%) |
| None | 58 (28.0%) | 19 (36.5%) | 87 (48.3%) |

(Continued)

TABLE 1 Continued

| Characteristic | Training cohort (n = 207) | Validation cohort (n = 52) | External validation cohort (n = 180) |
|---|---------------------------|----------------------------|--------------------------------------|
| Vascular pattern, n (%) | | | |
| Avascular | 129 (62.3%) | 24 (46.2%) | 71 (39.4%) |
| Peripheral or mixed | 78 (37.7%) | 28 (53.8%) | 109 (60.6%) |
| Calcification, n (%) | | | |
| Present | 204 (98.6%) | 50 (96.2%) | 172 (95.6%) |
| None | 3 (1.4%) | 2 (3.8%) | 8 (4.4%) |
| Surgery | | | |
| MIP | 169 (81.6%) | 42 (80.8%) | 160 (88.9%) |
| Bilateral neck exploration (BNE) + parathyroid adenoma excision | 12 (5.8%) | 3 (5.8%) | 4 (2.2%) |
| En bloc resection | 26 (12.6%) | 7 (12.4%) | 16 (8.9%) |
| Pathological subtype, n (%) | | | |
| Parathyroid adenoma | 181 (87.4%) | 41 (78.9%) | 165 (91.7%) |
| Atypical parathyroid tumors | 24 (11.6%) | 9 (17.3%) | 12 (6.7%) |
| parathyroid carcinoma | 2 (1.0%) | 2 (3.8%) | 3 (1.6%) |

iPTH, intact parathyroid hormone; MIP, minimally invasive parathyroidectomy; BNE, bilateral neck exploration.

cohort (n = 180). The rates of APT/PC in the training and validation cohorts [12.6% (26/207) and 21.1% (11/52), respectively] were not significantly different (p = 0.114). Vascular pattern and capsule showed a significant difference between the training and validation cohorts (p = 0.034, 0.010), and other indicators showed no difference between the two groups (P > 0.05). The ultrasound features showed good reproducibility and stability (ICC > 0.75), as described in [Supplementary Table S1](#).

3.2 Identification of predictive factors

The results of the univariate logistic regression analysis are presented in [Table 2](#). Variables with p < 0.2 were PTH (p < 0.001), serum calcium (p < 0.001), size (p < 0.001), echo texture (p = 0.026), shape (p < 0.001), composition (p = 0.011), relation with thyroid capsule (p = 0.003), and calcification (p = 0.002).

In the multivariate analysis, with results reported as odds ratio (OR) [95% confidence interval (CI)], PTH (1.019, 95% CI: 1.008–1.032), shape (16.625, 95% CI: 5.922–51.883), and relation with thyroid capsule (3.422, 95% CI: 1.455–9.152) were independent predictive factors associated with the risk of potentially malignant parathyroid diseases ([Table 3](#)).

TABLE 2 Univariate logistic regression analysis of potentially malignant parathyroid tumors in the training cohort.

| Characteristic | PA (n = 181) | APT/PC (n = 26) | p-value |
|--|----------------------|----------------------|--------------|
| Sex, n (%) | | | 0.258 |
| Male | 50 (27.6%) | 10 (38.5%) | |
| Female | 131 (72.4%) | 16 (61.5%) | 0.278 |
| Age at diagnosis, years | 57.00 (47.00, 65.00) | 57.50 (37.25, 62.75) | 0.519 |
| Serum iPTH, pmol/L [M (Q ₁ , Q ₃)] | 19.9 (13.5, 27.7) | 47.7 (32.1, 87.6) | <0.001 |
| Serum calcium, mmol/L [M (Q ₁ , Q ₃)] | 2.9 (2.7, 3.1) | 3.3 (3.0, 3.4) | <0.001 |
| Size, n (%) | | | |
| ≤3 cm | 139 (76.8%) | 10 (38.5%) | <0.001 |
| ≥3 cm | 42 (23.2%) | 16 (61.5%) | |
| Echo texture, n (%) | | | 0.026 |
| Hypochoic | 140 (77.3%) | 15 (57.7%) | |
| Hyperechoic | 7 (3.9%) | 1 (3.8%) | |
| Mixed | 34 (18.8%) | 10 (38.5%) | |
| Capsule, n (%) | | | 0.726 |
| Complete | 119 (65.7%) | 18 (69.2%) | |
| Incomplete | 62 (34.3%) | 8 (30.8%) | |
| Shape, n (%) | | | <0.001 |
| Regular | 160 (88.4%) | 8 (30.8%) | |
| Irregular | 21 (11.6%) | 18 (69.2%) | |
| Location, n (%) | | | |
| Typical | 167 (92.3%) | 26 (100%) | |
| Ectopic | 14 (7.7%) | 0 | |
| Composition, n (%) | | | 0.011 |
| Solid | 163 (90.1%) | 18 (69.2%) | |
| Cystic component ≤ 50% | 15 (8.3%) | 7 (26.9%) | |
| Cystic component > 50% | 3 (1.7%) | 1 (3.8%) | |
| Relation with thyroid capsule, n (%) | | | 0.003 |
| No-touching | 60 (33.1%) | 2 (7.7%) | |
| Indenting ≤ 50% | 92 (50.8%) | 6 (23.1%) | |
| Indenting > 50% | 29 (16.0%) | 18 (69.2%) | |
| Visualization of polar artery, n (%) | | | 0.087 |
| Present | 134 (74.0%) | 15 (57.7%) | |
| None | 47 (26.0%) | 11 (42.3%) | |

(Continued)

TABLE 2 Continued

| Characteristic | PA (n = 181) | APT/PC (n = 26) | p-value |
|--------------------------------|--------------|-----------------|------------------|
| Vascular pattern, n (%) | | | 0.343 |
| Avascular | 115 (63.5%) | 14 (53.8%) | |
| Peripheral or mixed | 66 (36.5%) | 12 (46.2%) | |
| Calcification, n (%) | | | <0.001 |
| Present | 0 | 23 (88.5%) | |
| None | 181 (100%) | 3 (11.5%) | |

PA, parathyroid adenoma; APT, atypical parathyroid tumor; PC, parathyroid cancer; iPTH, intact parathyroid hormone.

3.3 Nomogram construction and performance evaluation

These independent predictors were used to determine the risk of the APT/PC nomogram (Figure 3). To use the nomogram, the value of each patient was placed on each variable axis, and a line was drawn upward to determine the number of received points for each variable value. The sum of these numbers was located on the total point axis, and a line down the bottom axis was drawn to determine the probability of potentially malignant parathyroid tumors.

The model was validated both internally and externally by bootstrap validation. The nomogram demonstrated good accuracy for estimating the risk of aggressive parathyroid disease. The AUC for training, internal, and external validation was 0.929, 0.962, and 0.965, respectively. The accuracy, sensitivity, and specificity were 86%, 96%, and 85% in the training cohort; 92%, 100%, and 90% in the validation cohort; and 88%, 100%, and 88% in the external validation cohort, respectively (Table 4). In addition, calibration plots graphically showed good agreement on the presence of aggressive parathyroid diseases between risk estimation by the nomogram and histopathologic confirmation of surgical specimens. DCA in the current study showed that the nomogram of the aggressive parathyroid model used in our study was more effective than all-patient treatment or no treatment over a wide range of threshold probabilities (Figure 4).

4 Discussion

Our findings revealed three significant predictive factors: iPTH, shape, and relationship with thyroid capsule. We integrated three cohorts of patients with PHPT from two centers to develop and validate a nomogram based on the three predictive factors for parathyroid tumors. This nomogram enabled us to easily calculate the probability of APT/PC diagnosis, thereby facilitating early detection and appropriate treatment selection. This method prevents insufficient treatment, enhances patient outcomes, and minimizes the risk of complications from untreated or advanced tumors.

In our study, we identified statistically significant differences in size, echo texture, shape, composition, relation with the thyroid

TABLE 3 Multivariate logistic regression analysis of potentially malignant parathyroid tumors in the training cohort.

| Characteristic | Estimate | Std. Error | z-value | OR (95% CI) | p-value |
|-------------------------------|----------|------------|---------|------------------------|---------|
| iPTH | 0.019 | 0.006 | 3.278 | 1.019 (1.008, 1.032) | 0.001 |
| Shape | 2.811 | 0.548 | 5.134 | 16.625 (5.922, 51.883) | <0.001 |
| Relation with thyroid capsule | 1.231 | 0.464 | 2.649 | 3.422 (1.455, 9.152) | 0.008 |

PTH, intact parathyroid hormone; CI, confidence interval; OR, odds ratio.

capsule, calcification, and iPTH and serum calcium levels between the PA and APT/PC groups ($p < 0.05$). In the APT/PC group, 61.5% of the lesions exceeded 3 cm compared to 23.2% in the PA group, which is consistent with prior research (11). Malignancies often correspond to elevated serum iPTH and calcium levels and greater tumor weight than benign conditions (7, 22, 23). In our study, the iPTH level (OR: 1.019, 95% CI: 1.008–1.032) was an independent predictive factor associated with the risk of APT/PC. However, isolated iPTH levels are not reliable predictors of malignancy, as most lesions with excessive iPTH secretion are benign. PC rarely presents as normocalcemic hyperparathyroidism (24). Borderline iPTH excess might indicate compensation for vitamin D deficiency or low calcium intake, rather than PHPT. Therefore, malignancy prediction should consider this biochemical index, along with other sonographic risk factors.

On gross examination, PA usually presents as a well-defined, smooth, red-brown nodule with a thin capsule. Ultrasound imaging revealed well-defined oval to rounded or elongated homogeneously hypoechoic nodules. However, as parathyroid lesions increase in

size, echoic features can also vary. In a cohort of 907 patients with benign and atypical parathyroid adenomas, Hu et al. found an incidence of 4% for cystic parathyroid adenomas based on ultrasound or pathology. Interestingly, atypical adenomas are more common among cystic rather than solid lesions (25). The diagnosis of extensive cystic parathyroid neoplasms can be challenging because of the lack of hypersecretory behavior. These tumors may be incorrectly identified as thyroid cysts on scintigraphy, because they do not accumulate MIBI. Ultrasound is a critical diagnostic tool for differentiating between cystic and solid masses and for evaluating the risk of malignancy.

In our study, an irregular shape was observed in 69.2% of the patients in the PC/APT group and in 11.6% of the patients in the PA group. The irregular shapes include major lobulations, margin irregularities, and triangles. Shape (OR: 16.625, 95% CI: 5.922–51.883) was identified as an independent predictive factor of APT/PC risk. Additionally, Liu et al. (17) suggested that the “diameter ratio” can diagnose PC with 70.0% sensitivity, 91.7% specificity, 80.8% PPV, and 85.9% NPV. However, long-term secondary or

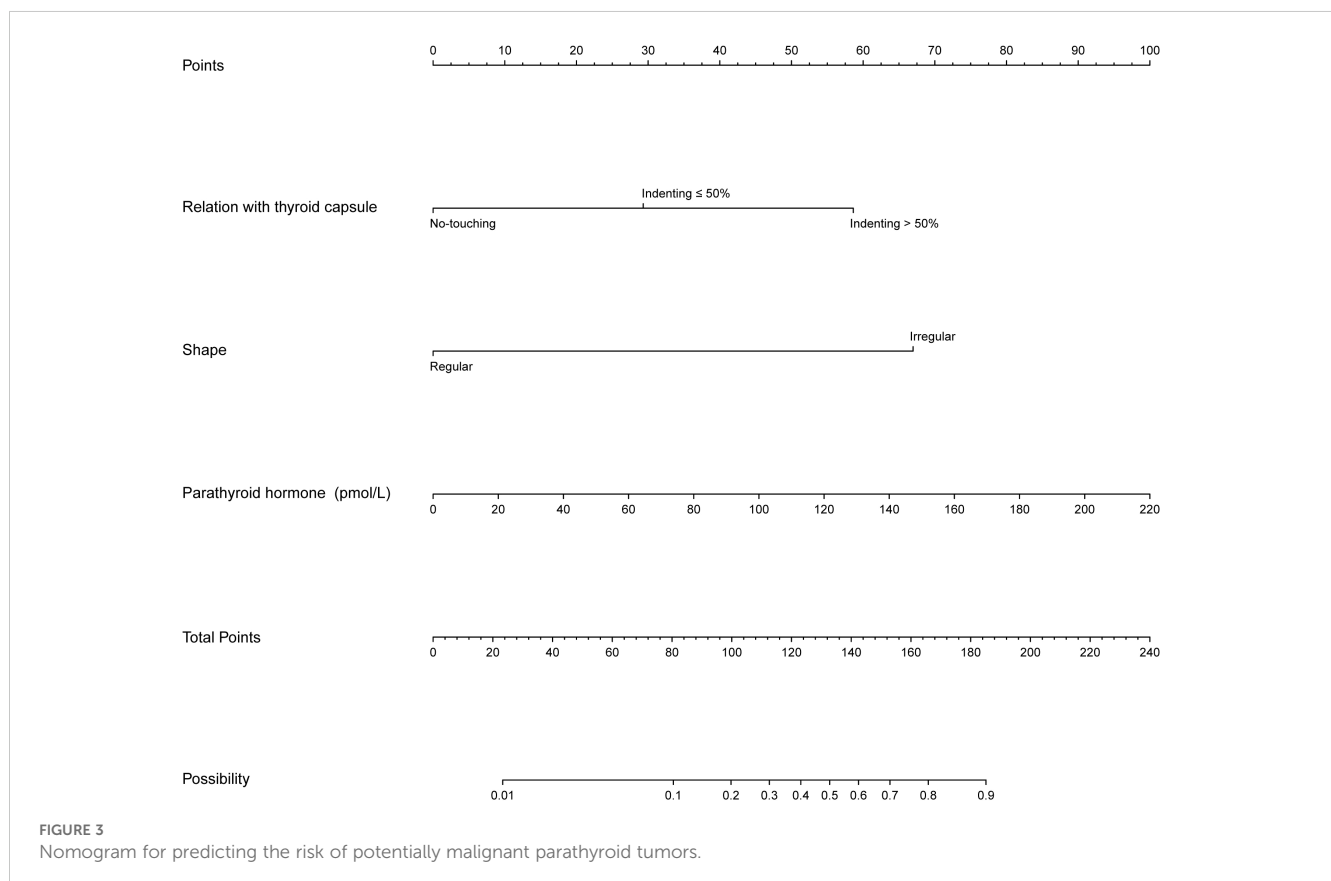


FIGURE 3 Nomogram for predicting the risk of potentially malignant parathyroid tumors.

TABLE 4 Accuracy of the prediction score of the nomogram for estimating the risk of aggressive parathyroid diseases.

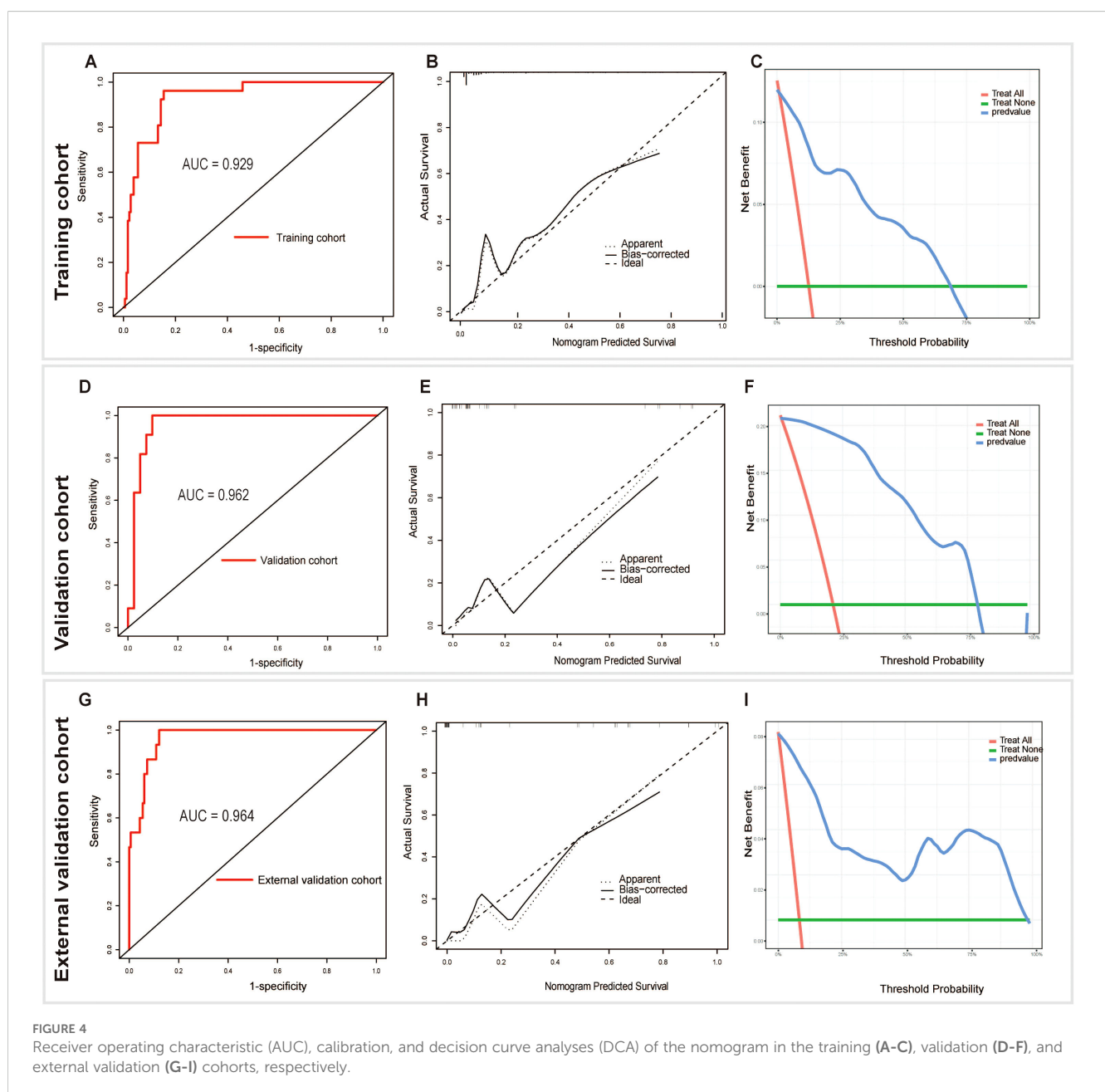
| | AUC (95% CI) | ACC (%) | SENS (%) | SPE (%) |
|----------------------------|----------------------|-------------|---------------|-------------|
| Training cohort | 0.929 (0.887, 0.973) | 86 (85, 87) | 96 (89, 100) | 85 (79, 90) |
| Validation cohort | 0.962 (0.913, 1.000) | 92 (91, 97) | 100 (96, 100) | 90 (81, 99) |
| External validation cohort | 0.965 (0.937, 0.992) | 88 (82, 89) | 100 (95, 100) | 88 (83, 93) |

AUC, area under the receiver operating characteristic curve; CI, confidence interval; ACC, accuracy; SEN, sensitivity; SPE, specificity.

tertiary hyperparathyroidism may result in enlarged parathyroid glands with irregular contours, which could mimic invasive growth. Therefore, caution should be exercised when diagnosing PC in patients with advanced chronic renal failure.

We also found that the relation with the thyroid capsule (OR: 3.422, 95% CI: 1.455–9.152) was an independent predictive factor

associated with the risk of APT/PC. The relation between the parathyroid mass and thyroid gland is close, which indirectly reflects the aggressiveness of parathyroid tumors. Malignant tumors often exhibit infiltrative growth and invade surrounding tissues. Under these circumstances, the capsular margins of both the parathyroid nodule and the adjacent thyroid are not clearly



identified, often rendering a demarcation of the cleavage plane between the thyroid and parathyroid gland.

Vascular information is crucial for diagnosing parathyroid nodules, with enlarged parathyroid glands exhibiting more hypervascularity than thyroid nodules. Hunter et al. highlighted that variations in tissue vascular pathophysiological parameters are essential for accurate localization of PAs using 4D-CT imaging (26). Liu et al. enhanced polar vessel detection and blood flow signal quantification using Angio Plus ultrasound imaging (27). Their study indicated that a visible polar artery strongly suggests a parathyroid lesion characterized by peripheral and central blood flow patterns. In line with our findings, 74.0% of patients (134 of 181) in the PA group showed polar artery visualization. However, the presence of the polar artery was not unique to PA, as demonstrated by the 57.7% visualization rate (15 of 26) in the APT/PC group. Some parathyroid neoplasms may be associated with complete or incomplete encapsulation, while there were no significant differences between the two groups in terms of the capsule in our study. This may be due to the small sample size in the APT/PC group. Incomplete encapsulation may be relevant to intraoperative adhesion and invasion of the adjacent capsule. Speaking of calcification, Shah et al. found that intratumoral calcification had 100% positive predictive value to diagnose PC on PHPT (28).

In the absence of standardized clinical guidelines for preoperative risk stratification of PC in patients with PHPT, individuals undergoing localized parathyroidectomy frequently lack systematic oncological risk evaluations. This oversight may result in suboptimal surgical interventions that inadequately address malignant potential (7). Our retrospective cohort analysis of 439 patients with parathyroid pathologies identified 7 confirmed PC cases and 45 APT cases. Among these, 49 patients (11.2%) underwent *en bloc* resection due to intraoperative findings of extensive adhesions or concurrent suspicion of malignant thyroid nodules. Historically, intraoperative decision-making at our institution relied predominantly on macroscopic adhesion severity or intraoperative frozen section results suggestive of malignancy. To address this limitation, we proposed a novel risk stratification framework for parathyroid lesions, integrating clinical and ultrasonic predictors to categorize patients into distinct therapeutic cohorts. Predictive modeling via nomogram analysis demonstrated that preoperative *en bloc* resection would have been appropriately indicated in a minimum of 56/439 patients (12.8%) with suspected APT/PC, potentially reducing recurrence risk through optimized radical resection margins. However, the diagnostic performance evaluation revealed a consistent trend of modestly reduced specificity (range: 85%–90%) relative to sensitivity (96%–100%) across the three datasets, indicating a nonnegligible false-positive rate. This diagnostic asymmetry raises concerns regarding overtreatment, which may impose unnecessary morbidity and healthcare burdens on patients with indolent pathologies.

This study had several limitations. First, this retrospective study excluded recurrent PHPT and SHPT; hence, the model had potential selection bias. Second, ultrasound findings, including

tumor size and margins, were subjectively assessed by a sonographer. These subjective assessments, unlike objective factors such as age and iPTH level, could significantly influence the final nomogram results, posing a critical issue for clinical application in evaluating potential tumors. To mitigate this limitation, standardized ultrasound assessment protocols were established, and interobserver agreement and intraobserver agreement in the evaluation of radiological features were calculated. Future studies could incorporate artificial intelligence-based image analysis techniques, which could potentially provide more objective and consistent evaluations of tumor characteristics. Third, the sample sizes were small across various cohorts owing to the rarity of PC or APT cases. Fourth, this study only considered the ultrasound manifestations. Prospective cohort studies with more imaging modalities (e.g., sestamibi scans, CT, or MRI), larger sample sizes, and multiple centers are required to improve diagnostic accuracy for parathyroid lesions. Fifth, serum PTH testing may have an impact on the accuracy of our PTH measurements, which could significantly influence the nomogram validity. This study spans an era of evolving PTH assay technologies. Although all measurements utilized second-generation assays targeting intact PTH (1–84), platform transitions (e.g., from Centaur XP to Atellica IM) and reagent lot variations may introduce non-quantified inter-assay variability. In fact, we are in progress to establish a prospective study of APC/PC, and the new data may shed light on the problems mentioned above.

In summary, we developed and validated a nomogram to improve preoperative diagnosis of parathyroid lesions. This diagnostic tool can aid clinicians in identifying patients at a higher risk of developing APT/PC, potentially leading to more appropriate management and follow-up strategies.

Data availability statement

The raw data supporting the conclusions of this article will be made available by the authors, without undue reservation.

Ethics statement

The studies involving humans were approved by Nanjing Drum Tower Hospital Ethics Committee (2024-611-01). The studies were conducted in accordance with the local legislation and institutional requirements. The participants provided their written informed consent to participate in this study.

Author contributions

CL: Conceptualization, Data curation, Formal Analysis, Methodology, Writing – original draft. ML: Data curation, Methodology, Supervision, Validation, Writing – review & editing. WL: Data curation, Validation, Visualization, Writing – review & editing. HX: Investigation, Methodology, Writing – review & editing.

YZ: Investigation, Methodology, Writing – review & editing. SW: Formal Analysis, Supervision, Validation, Writing – review & editing. JH: Resources, Validation, Visualization, Writing – review & editing. JY: Funding acquisition, Resources, Supervision, Validation, Visualization, Writing – review & editing. ZZ: Funding acquisition, Methodology, Project administration, Visualization, Writing – review & editing.

Funding

The author(s) declare that financial support was received for the research and/or publication of this article. This work was supported by the National Natural Science Foundation (81771844 and 82371981).

Conflict of interest

The authors declare that the research was conducted in the absence of any commercial or financial relationships that could be construed as a potential conflict of interest.

References

- Sun B, Guo B, Wu B, Kang J, Deng X, Zhang Z, et al. Characteristics, management, and outcome of primary hyperparathyroidism at a single clinical center from 2005 to 2016. *Osteoporos Int.* (2018) 29:635–42. doi: 10.1007/s00198-017-4322-7
- Erickson LA, Mete O, Juhlin CC, Perren A, Gill AJ. Overview of the 2022 WHO classification of parathyroid tumors. *Endocr Pathol.* (2022) 33:64–89. doi: 10.1007/s12022-022-09709-1
- Reid L, Muthukrishnan B, Patel D, Crane M, Akyol M, Thomson A, et al. Presentation, diagnostic assessment and surgical outcomes in primary hyperparathyroidism: a single centre's experience. *Endocr Connect.* (2018) 7:1105–15. doi: 10.1530/EC-18-0195
- Rodrigo JP, Hernandez-Prera JC, Randolph GW, Zafereo ME, Hartl DM, Silver CE, et al. Parathyroid cancer: an update. *Cancer Treat Rev.* (2020) 86:102012. doi: 10.1016/j.ctrv.2020.102012
- Bilezikian JP, Cusano NE, Khan AA, Liu J-M, Marcocci C, Bandeira F. Primary hyperparathyroidism. *Nat Rev Dis Primers.* (2016) 2:16033. doi: 10.1038/nrdp.2016.33
- Zhao L, Liu J-M, He X-Y, Zhao H-Y, Sun L-H, Tao B, et al. The changing clinical patterns of primary hyperparathyroidism in Chinese patients: data from 2000 to 2010 in a single clinical center. *J Clin Endocrinol Metab.* (2013) 98:721–8. doi: 10.1210/jc.2012-2914
- Schulte K-M, Talat N. Diagnosis and management of parathyroid cancer. *Nat Rev Endocrinol.* (2012) 8:612–22. doi: 10.1038/nrendo.2012.102
- Cetani F, Pardi E, Marcocci C. Update on parathyroid carcinoma. *J Endocrinol Invest.* (2016) 39:595–606. doi: 10.1007/s40618-016-0447-3
- Silva-Figueroa AM, Bassett R, Christakis I, Moreno P, Clarke CN, Busaidy NL, et al. Using a novel diagnostic nomogram to differentiate Malignant from benign parathyroid neoplasms. *Endocr Pathol.* (2019) 30:285–96. doi: 10.1007/s12022-019-09592-3
- Gurrado A, Pasculli A, Avenia N, Bellantone R, Boniardi M, Merante Boschin I, et al. Parathyroid retrospective analysis of neoplasms incidence (pTRANI Study): an Italian multicenter study on parathyroid carcinoma and atypical parathyroid tumour. *JCM.* (2023) 12:6297. doi: 10.3390/jcm12196297
- Kakir B, Polat SB, Kilic M, Ozdemir D, Aydin C, Süngü N, et al. Evaluation of preoperative ultrasonographic and biochemical features of patients with aggressive parathyroid disease: is there a reliable predictive marker? *Arch Endocrinol Metab.* (2016) 60:537–44. doi: 10.1590/2359-3997000000224
- Schouw HM, Noltes ME, Brouwers AH, Nilsson I-L, Zedenius J, Kruijff S. How nuclear imaging changed parathyroid surgical strategies through time. *Eur J Nucl Med Mol Imaging.* (2024) 51:2165–71. doi: 10.1007/s00259-024-06707-9

Generative AI statement

The author(s) declare that no Generative AI was used in the creation of this manuscript.

Publisher's note

All claims expressed in this article are solely those of the authors and do not necessarily represent those of their affiliated organizations, or those of the publisher, the editors and the reviewers. Any product that may be evaluated in this article, or claim that may be made by its manufacturer, is not guaranteed or endorsed by the publisher.

Supplementary material

The Supplementary Material for this article can be found online at: <https://www.frontiersin.org/articles/10.3389/fendo.2025.1538361/full#supplementary-material>

- Singhal AA. *Atlas of Sonography of Parathyroid*. Singapore: Springer Nature Singapore (2023). doi: 10.1007/978-981-19-7919-4
- Zhang M, Sun L, Rui W, Guo R, He H, Miao Y, et al. Semi-quantitative analysis of 99mTc-sestamibi retention level for preoperative differential diagnosis of parathyroid carcinoma. *Quant Imaging Med Surg.* (2019) 9:1394–401. doi: 10.21037/qims.2019.07.02
- Greene C, Fujima N, Sakai O, Andreu-Arasa VC. Comparing accuracy of machine learning approaches to identifying parathyroid adenomas: Lessons and new directions. *Am J Otolaryngol.* (2024) 45:104155. doi: 10.1016/j.amjoto.2023.104155
- Boudousq V, Guignard N, Gilly O, Chambert B, Mamou A, Moranne O, et al. Diagnostic performance of cervical ultrasound, ^{99m}Tc-Sestamibi scintigraphy, and contrast-enhanced ¹⁸F-Fluorocholine PET in primary hyperparathyroidism. *J Nucl Med.* (2022) 63:1081–6. doi: 10.2967/jnumed.121.261900
- Liu R, Xia Y, Chen C, Ye T, Huang X, Ma L, et al. Ultrasound combined with biochemical parameters can predict parathyroid carcinoma in patients with primary hyperparathyroidism. *Endocrine.* (2019) 66:673–81. doi: 10.1007/s12020-019-02069-7
- Liu R, Gao L, Shi X, Ma L, Wang O, Xia W, et al. Shear wave elastography for differentiating parathyroid neoplasms with Malignant diagnosis or uncertain Malignant potential from parathyroid adenomas: initial experience. *Cancer Imaging.* (2022) 22:64. doi: 10.1186/s40644-022-00503-0
- Zhou W, Zhou Y, Zhang X, Huang T, Zhang R, Li D, et al. Development and validation of an explainable machine learning model for identification of hyperfunctioning parathyroid glands from high-frequency ultrasonographic images. *Ultrasound Med Biol.* (2024) 50:1506–14. doi: 10.1016/j.ultrasmedbio
- Ilgan S, Aydoğan Bİ, Emer Ö, Anil C, Gürsoy A, Cesur M, et al. Sonographic features of atypical and initially missed parathyroid adenomas: lessons learned from a single-center cohort. *J Clin Endocrinol Metab.* (2024) 109:439–48. doi: 10.1210/clinem/dgad527
- Yazgi D, Richa C, Salenave S, Kamenicky P, Bourouina A, Clavier L, et al. Differentiating pathologic parathyroid glands from thyroid nodules on neck ultrasound: the PARATH-US cross-sectional study. *Lancet Reg Health Eur.* (2023) 35:100751. doi: 10.1016/j.lanepe.2023.100751
- Filser B, Uslar V, Weyhe D, Tabriz N. Predictors of adenoma size and location in primary hyperparathyroidism. *Langenbecks Arch Surg.* (2021) 406:1607–14. doi: 10.1007/s00423-021-02179-9
- Williams MD, DeLellis RA, Erickson LA, Gupta R, Johnson SJ, Kameyama K, et al. Pathology data set for reporting parathyroid carcinoma and atypical parathyroid neoplasm: recommendations from the International Collaboration on Cancer Reporting. *Hum Pathol.* (2021) 110:73–82. doi: 10.1016/j.humpath.2020.07.008

24. Campenni A, Ruggeri RM. Early diagnosis of parathyroid carcinoma: A challenging for physicians. *Clin Endocrinol (Oxf)*. (2023) 98:273–4. doi: 10.1111/cen.14807
25. Hu Y, Cui M, Xia Y, Su Z, Zhang X, Liao Q, et al. The clinical features of cystic parathyroid adenoma in Chinese population: a single-center experience. *Int J Endocrinol*. (2018) 2018:1–6. doi: 10.1155/2018/3745239
26. Hunter GJ, Ginat DT, Kelly HR, Halpern EF, Hamberg LM. Discriminating parathyroid adenoma from local mimics by using inherent tissue attenuation and vascular information obtained with four-dimensional CT: formulation of a multinomial logistic regression model. *Radiology*. (2014) 270:168–75. doi: 10.1148/radiol.13122851
27. Liu H, Liao Q, Wang Y, Hu Y, Zhu Q, Wang L, et al. A new tool for diagnosing parathyroid lesions: angio plus ultrasound imaging. *J Thorac Dis*. (2019) 11:4829–34. doi: 10.21037/jtd.2019.11.29
28. Shah R, Gosavi V, Mahajan A, Sonawane S, Hira P, Kurki V, et al. Preoperative prediction of parathyroid carcinoma in an Asian Indian cohort. *Head Neck*. (2021) 43:2069–80. doi: 10.1002/hed.26677